Received 28 December 2001; accepted 6 February 2002.

1. Hicke, L. A new ticket for entry into budding vesicles—ubiquitin. *Cell* **106,** 527–530 (2001).
2. Weissman, A. M. Themes and variations on ubiquitination. *Nature Rev. Mol. Cell Biol.* **2,** 169–178 (2001).
3. Hicke, L. Protein regulation by monoubiquitin. *Nature Rev. Mol. Cell Biol.* **2,** 195–201 (2001).
4. Laney, J. D. & Hochstrasser, M. Substrate targeting in the ubiquitin system. *Cell* **97,** 427–430 (1999).
5. Katzmann, D. J., Babst, M. & Emr, S. D. Ubiquitin-dependent sorting into the multivesicular body pathway requires the function of a conserved endosomal protein sorting complex, ESCRT-I. *Cell* **106,** 145–155 (2001).
6. Hofmann, K. & Falquet, l. A ubiquitin-interacting motif conserved in components of the proteasomal and lysosomal protein degradation systems. *Trends Biochem. Sci.* **26,** 347–350 (2001).
7. van Delft, S., Govers, R., Strous, G J., Verkleij, A. J. & van Bergen en Henegouwen, P. M. Epidermal growth factor induces ubiquitination of Eps15. *J. Biol. Chem.* **272,** 14013–14016 (1997).
8. Coda, L. *et al.* Eps15R is a tyrosine kinase substrate with characteristics of a docking protein possibly involved in coated pits-mediated internalization. *J. Biol. Chem.* **273,** 3003–3012 (1998).
9. Santolini, E., Salcini, A. E., Kay, B. K., Yamabhai, M. & Di Fiore, P. P. The EH network. *Exp. Cell Res.* **253,** 186–209 (1999).
10. Wong, W. T. *et al.* A protein-binding domain, EH, identified in the receptor tyrosine kinase substrate Eps15 and conserved in evolution. *Proc. Natl Acad. Sci. USA* **92,** 9530–9534 (1995).
11. Benmerah, A., Begue, B., Dautry-Varsat, A. & Cerf-Bensussan, N. The ear of alpha-adaptin interacts with the COOH-terminal domain of the Eps15 protein. *J. Biol. Chem.* **271,** 12111–12116 (1996).
12. Iannolo, G. *et al.* Mapping of the molecular determinants involved in the interaction between eps15 and AP-2. *Cancer Res.* **57,** 240–245 (1997).
13. Chen, H. *et al.* Epsin is an EH-domain-binding protein implicated in clathrin-mediated endocytosis. *Nature* **394,** 793–797 (1998).
14. Komada, M. & Kitamura, N. Growth factor-induced tyrosine phosphorylation of Hrs, a novel 115-kilodalton protein with a structurally conserved putative zinc finger domain. *Mol. Cell Biol.* **15,** 6213–6221 (1995).
15. Young, P., Deveraux, Q., Beal, R. E., Pickart, C. M. & Rechsteiner, M. Characterization of two polyubiquitin binding sites in the 26 S protease subunit 5a. *J. Biol. Chem.* **273,** 5461–5467 (1998).
16. van Nocker, S. *et al.* The multiubiquitin-chain-binding protein Mcb1 is a component of the 26S proteasome in *Saccharomyces cerevisiae* and plays a nonessential, substrate-specific role in protein turnover. *Mol. Cell Biol.* **16,** 6020–6028 (1996).
17. Beal, R., Deveraux, Q., Xia, G., Rechsteiner, M. & Pickart, C. Surface hydrophobic residues of multiubiquitin chains essential for proteolytic targeting. *Proc. Natl Acad. Sci. USA* **93,** 861–866 (1996).
18. Deveraux, Q., Ustrell, V., Pickart, C. & Rechsteiner, M. A 26S protease subunit that binds ubiquitin conjugates. *J. Biol. Chem.* **269,** 7059–7061 (1994).
19. Huibregtse, J. M., Scheffner, M., Beaudenon, S. & Howley, P. M. A family of proteins structurally and functionally related to the E6-AP ubiquitin-protein ligase. *Proc. Natl Acad. Sci. USA* **92,** 2563–2567 (1995).
20. Staub, O. *et al.* WW domains of Nedd4 bind to the proline-rich PY motifs in the epithelial Na^+ channel deleted in Liddle's syndrome. *EMBO J.* **15,** 2371–2380 (1996).
21. Wang, G. *et al.* Localization of the Rsp5p ubiquitin-protein ligase at multiple sites within the endocytic pathway. *Mol. Cell Biol.* **21,** 3564–3575 (2001).
22. Dunn, R. & Hicke, L. Multiple roles for Rsp5p-dependent ubiquitination at the internalization step of endocytosis. *J. Biol. Chem.* **276,** 25974–25981 (2001).
23. Dunn, R. & Hicke, L. Domains of the Rsp5 ubiquitin-protein ligase required for receptor-mediated and fluid-phase endocytosis. *Mol. Biol. Cell* **12,** 421–435 (2001).
24. Gagny, B. *et al.* A novel EH domain protein of *Saccharomyces cerevisiae*, Ede1p, involved in endocytosis. *J. Cell. Sci.* **113,** 3309–3319 (2000).
25. Jensen, J. P., Bates, P. W., Yang, M., Vierstra, R. D. & Weissman, A. M. Identification of a family of closely related human ubiquitin conjugating enzymes. *J. Biol. Chem.* **270,** 30408–30414 (1995).
26. Itoh, T. *et al.* Role of the ENTH domain in phosphatidyl inositol-4,5-bisphosphate binding and endocytosis. *Science* **291,** 1047–1051 (2001).
27. Patki, V., Lawe, D. C., Corvera, AS., Virbasius, J. V. & Chawla, A. A functional PtdIns(3)P-binding motif. *Nature* **394,** 433–434 (1998).
28. Burd, C. G. & Emr, S. D. Phosphatidylinositol(3)-phosphate signaling mediated by specific binding to RING FYVE domains. *Mol. Cell* **2,** 157–162 (1998).
29. Gaullier, J. M. *et al.* FYVE fingers bind PtdIns(3)P. *Nature* **394,** 432–433 (1998).
30. Avantaggiati, M. L. *et al.* The SV40 large T antigen and adenovirus E1a oncoproteins interact with distinct isoforms of the transcriptional co-activator, p300. *EMBO J.* **15,** 2236–2248 (1996).

Supplementary Information accompanies the paper on *Nature's* website (http://www.nature.com).

Acknowledgements

We thank H. Asao and A. Bean for Hrs constructs, I. Berdo for E1 purification, G. F. Draetta for UbcH5B, Nedd4 and His-Ub constructs, M. Sudol for γEnaC constructs, and G. Gill for B82L cells. We thank A. Musacchio for comments that improved the manuscript. We also thank S. Confalonieri for assistance with biocomputing. This work was supported by grants from the Associazione Italiana Ricerca sul Cancro, the Telethon Foundation, the CNR (Progetto Biotecnologie), and the EC (V framework).

Competing interests statement

The authors declare that they have no competing financial interests.

Correspondence and requests for materials should be addressed to P.P.D.F. (e-mail: pdifiore@ieo.it).

Crystal structure of DegP (HtrA) reveals a new protease-chaperone machine

Tobias Krojer*†, Marta Garrido-Franco*, Robert Huber*, Michael Ehrmann† & Tim Clausen*

** Max-Planck-Institut für Biochemie, Abteilung Strukturforschung, Am Klopferspitz 18A, 82152 Martinsried, Germany*
† Cardiff University, School of Biosciences, Museum Avenue, Cardiff CF10 3US, UK

Molecular chaperones and proteases monitor the folded state of other proteins. In addition to recognizing non-native conformations, these quality control factors distinguish substrates that can be refolded from those that need to be degraded[1]. To investigate the molecular basis of this process, we have solved the crystal structure of DegP (also known as HtrA), a widely conserved heat shock protein that combines refolding and proteolytic activities[2]. The DegP hexamer is formed by staggered association of trimeric rings. The proteolytic sites are located in a central cavity that is only accessible laterally. The mobile sidewalls are constructed by twelve PDZ domains, which mediate the opening and closing of the particle and probably the initial binding of substrate. The inner cavity is lined by several hydrophobic patches that may act as docking sites for unfolded polypeptides. In the chaperone conformation, the protease domain of DegP exists in an inactive state, in which substrate binding in addition to catalysis is abolished.

Problems associated with protein folding need to be addressed by all living cells. Molecular chaperones and proteases control the folded state of proteins by recognizing hydrophobic stretches of polypeptides that become exposed by misfolding or unfolding. Molecular chaperones either simply bind substrates to prevent aggregation, or they actively assist in refolding. If attempts at refolding fail, irreversibly damaged proteins are degraded by proteases[1]. Despite extensive research into protease and chaperone mechanisms, the control of this editing function is poorly understood. While most factors involved in protein quality control are ATP-dependent heat shock proteins[3], DegP fulfils this role without consuming ATP[4]. DegP is a widely conserved extracytoplasmic protein that switches from chaperone to protease in a temperature-dependent manner[2], the protease activity being most apparent at elevated temperatures. Prokaryotic DegP proteins have been attributed to the tolerance against various folding stresses as well as to pathogenicity[5]. Human homologues are believed to be involved in arthritis, cell growth, unfolded protein response and apoptosis[6–8]. Our described structural study of *Escherichia coli* DegP is a start towards dissecting the molecular mechanism of this quality control factor, providing the required stereochemical framework for further genetic, biochemical, and biophysical studies. The unique structural organization of the DegP hexamer indicates a new type of protease-chaperone machine.

Native DegP undergoes slow self cleavage. Thus we used a proteolytically inactive mutant for structural determination, in which the active site serine was replaced by alanine (S210A). After successful crystallization at room temperature, the hexagonal crystals were transferred to 4 °C, thereby locking the protein in the 'chaperone conformation'. In the asymmetric unit of the crystals, two DegP molecules were observed, which we refer to here as A and B. The DegP monomer can be divided into three functionally distinct domains, namely a protease (residues 1–259) and two PDZ domains (PDZ1, residues 260–358; PDZ2, residues 359–448) (Fig. 1a). The previously proposed amino-terminal domain[5] con-

tributes to the protease fold. Part of this N-terminal segment, the 'Q-linker'[9] (residues 55–79), was too flexible to be traced in the electron density. Similar to other members of the trypsin family, the protease domain of DegP has two perpendicular β-barrel lobes with a carboxy-terminal helix. The catalytic triad is located in the crevice between the two lobes. The overall fold of the two PDZ domains is similar to other PDZ domains of known structure[10,11]; however, PDZ1 has β13 and αf as additional elements, which are important for the subunit interactions within the DegP hexamer. Interestingly, the PDZ1 domains are arranged differently in molecules A and B, whereas PDZ2 was only defined by electron density in molecule B. Although these differences may be influenced by crystal packing constraints, the pronounced mobility of the PDZ domains seems to be mechanistically important. The overall conformations of the protease (including the N terminus) and the PDZ1 domains are otherwise identical. When aligned separately, the root-mean-squared deviation (r.m.s.d.) of the Cα atoms of the protease domain was 0.54 Å, whereas the r.m.s.d. between the individual PDZ1 domains was 1.33 Å.

The DegP A and B hexamers are centred in the crystallographic unit cell at (0, 0, 0) and (2/3, 1/3, 1/4), respectively, and display crystallographic D3 symmetry. Crystal contacts are observed between the protease parts of A and B. The PDZ domains do not contribute to packing (see Supplementary Information Fig. 1). Notably, the observed hexamers represent two distinct states. Molecule A is a largely open structure with a wide lateral passage penetrating the entire oligomer, whereas molecule B corresponds to the closed form, in which a triangle-shaped 45 Å cavity containing the proteolytic sites is completely shielded from solvent (Fig. 1b). For both molecules A and B, the top and bottom of the DegP cage are constructed by the six protease domains, whereas the 12 PDZ domains generate the mobile side-walls. Because the axial pores of

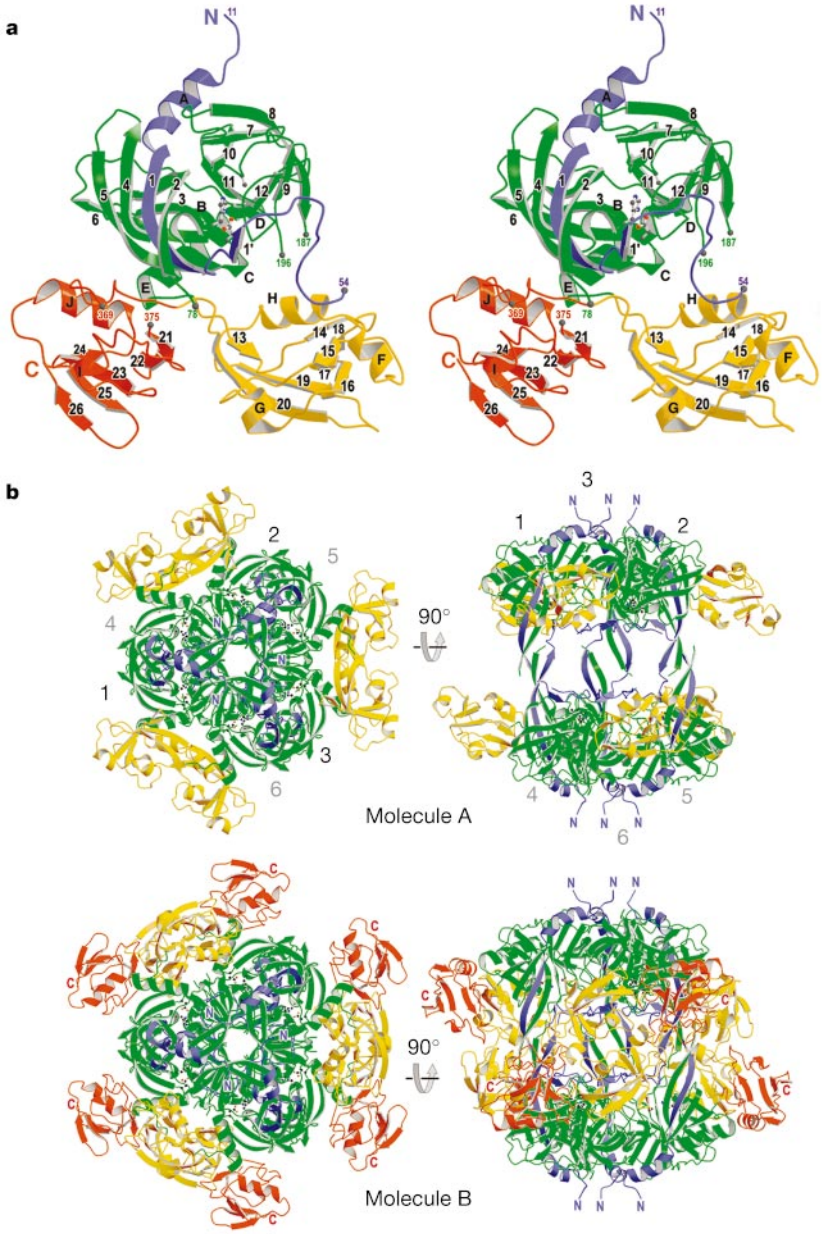

Figure 1 Structure of DegP. **a**, Stereo ribbon presentation of the monomer in which the individual domains are coloured differently. N terminal, purple; protease, green; PDZ1, yellow; PDZ2, red. Residues of the catalytic triad are shown in a ball-and-stick model. The nomenclature of secondary structure elements (helices by letter, strands by numbers), the termini of the protein, and regions that were not defined by electron density are indicated. **b**, Top and side views of the DegP hexamer constructed by molecules A and B. Both hexamers are approximately equal in size, having a height of 105 Å and a diameter of 120 Å. The nomenclature of the individual monomers and their termini are given.

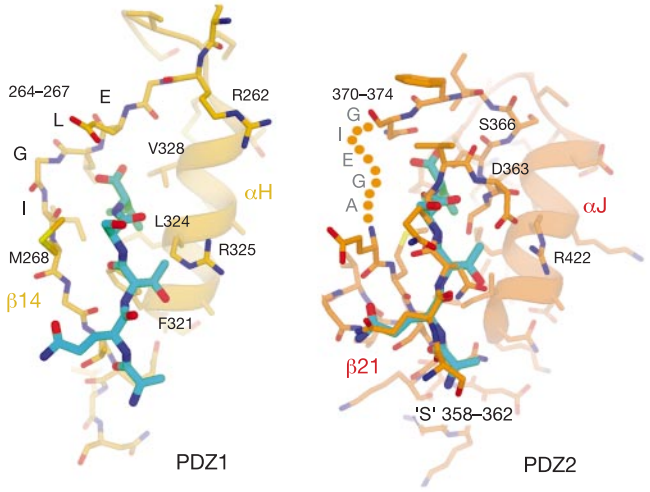

Figure 2 Peptide-binding sites of PDZ1 and PDZ2. The bordering β-strand, α-helix and carboxylate-binding loop are shown in a stick model and are coloured by atom type. After superposition with complexed PSD95, the peptide ligand (cyan) was modelled into the binding sites of both of the PDZ domains. Residues that may participate in substrate binding (PDZ1) and residues that anchor the substrate-like segment ('S', PDZ2) are labelled. The G-I-E-G-A motif of PDZ2 was not defined in the electron density, as indicated by the dashed coil.

the particle are blocked completely, the PDZ domains are the only gates allowing lateral access to the central cavity. This structural organization is markedly different from other cage-forming proteins, where substrates enter the central cavity through narrow axial or lateral pores[12–17]. In particular, the PDZ1 domains interact with each other and should thus be the main gatekeepers of the inner chamber. The height of the cavity is determined by three molecular pillars, which are formed by enlarged loops of the protease domain. These pillars are also mainly responsible for the stability of the dynamic complex as seen in the open state.

The contacts between trimeric rings of the DegP hexamer arise almost exclusively from highly flexible structural elements. Thus, the DegP hexamer should be considered as a loosely bound dimer of tight trimers. Monomers associate into trimers mainly by hydrophobic interactions. The resulting trimeric rings interact through the polar 1–4 and 1–6 interfaces (Fig. 1b). In the 1–4 interface, the enlarged protease loops termed LA (connecting β1 and β2) are wound around each other and build the corner pillars of the DegP cage. This molecular spacer is mainly stabilized by the two-stranded β-sheet 1′/2* (the asterisk denotes the participation of the neighbouring monomer). After reaching the opposite ceiling of the cavity, loop LA protrudes into the active site of its partner subunit. In the hexamer of molecule B, the 1–6 interface is formed by the interaction of PDZ1 and PDZ2 with their symmetry mates. The PDZ domains obtain a zipper-like arrangement, in which the PDZ1 domains are facing each other, whereas the PDZ2 domains are bound at their edges. Residues of this interface originate from the αF-β15-αG segment (PDZ1) and from β22-αI (PDZ2). In the open form of molecule A, PDZ1 tilts 70° away, thereby moving the αF-β15-αG interaction clamp to the opposite side of the trimer–trimer interface (corresponding to a 30 Å movement), and breaking the 1–6 subunit interaction. The re-orientation of PDZ1 is achieved by a twist of the polypeptide backbone between residues Arg 262 and Gly 263.

In addition to their function in regulating access to the inner cavity, the PDZ domains of DegP should be involved in substrate binding. To identify the determinants of substrate specificity of PDZ1 and PDZ2, we aligned both structures with the peptide complex of the PDZ protein PSD95 (ref. 18), and modelled the bound ligand to both PDZ domains of DegP (Fig. 2). PDZ1 contains a deep binding cleft for substrate, which is mainly constructed by strand 14, its N-terminal loop (the 'carboxylate-binding loop'), and helix H. The carboxylate-binding loop is located in a highly positively charged region and is formed by an E-L-G-I motif, which is similar to the frequently observed G-L-G-F motif[10]. The side-chain of the strictly conserved Arg 262 is properly oriented to further fix the carboxylate group of the substrate. As this arginine is one of the hinge residues connecting protease and PDZ1, substrate binding to Arg 262 might trigger re-orientation of the PDZ domain. Binding specificity is conferred mainly by the specific configuration of the 0, −2 and −3 binding pockets[19], where pocket 0 anchors the side chain of the C-terminal residue. In PDZ1, all pockets are built by residues that are mainly hydrophobic (Supplementary Information Fig. 2). One of the main differences to other PDZ domains is the flexibility of strand 14 and its associated carboxylate-binding loop, indicating the plasticity of the binding site. Thus PDZ1 seems to be well adapted to bind various stretches of hydrophobic peptide ligands.

The comparison between PSD95 and PDZ2 suggests a new mechanism of substrate binding and release. In PDZ2, the loop consisting of residues 355–369 adopts a conformation that mimics a bound substrate molecule (Fig. 2). Residues 358–362 are bound in extended conformation antiparallel to β-strand 21, and several specific interactions occur with helix J. This substrate-like segment

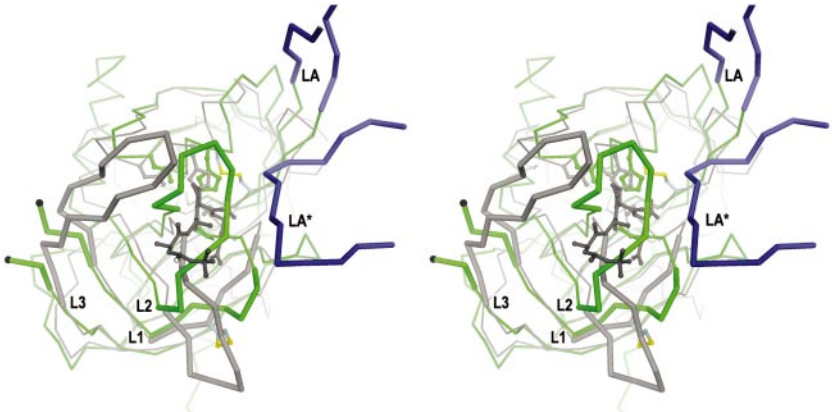

Figure 3 The protease domain. Structural alignment of the DegP protease domain (green and blue) with SGT (grey). In the stereo image, both backbones are shown as a Cα trace, whereas the catalytic triads, the peptide bound to SGT (brown) and its disulphide bridges are drawn in ball-and-stick mode. Some of the mechanistically important loops (L1, L2, L3 and LA* (ref. 30)) are emphasized by thicker lines and are labelled. Note that loop LA* (blue) originates from the partner monomer. Loop L3 of DegP was only partially defined in the electron density.

is connected by the carboxylate-binding loop (comprising the G-I-E-G-A motif) to the remainder of PDZ2. The highly flexible carboxylate-binding loop might allow re-orientation of the substrate-like segment, and thereby the opening and closing of the peptide-binding site. As the occluded pocket was observed in the closed form of the DegP cage, displacement of a bound substrate by the loop 355–369 might be involved in the process of substrate translocation. As for PDZ1, some of the structural elements that might be involved in substrate binding, that is, the carboxylate-binding loop and strand 21, have considerably higher thermal motion factors than the rest of the domain, pointing again to a flexible binding site. Thus, both PDZ domains represent two forms of flexibility: a rigid-body movement generated by different twists of the hinge regions, and a local flexibility that should enable the accommodation of a wide range of substrates. Consequently, the PDZ domains are good candidates for the initial interaction with substrate.

The Dali algorithm was used to search for structural homologues of the protease domain. *Streptomyces griseus* trypsin (SGT), epidermolytic toxin, β-trypsin and thrombin were identified as the most similar structures in the database (Supplementary Information Table 1). Although the core of the protease domain is highly conserved, there are marked differences in the surface loops, which are important for the adjustment of the catalytic triad (Asp 105, His 135, Ser 210) and the specificity pocket S1 (Fig. 3). The enlarged loop LA protrudes into the active site of one monomer of the opposite trimeric ring, where it intimately interacts with loops L1 and L2. The resulting loop triad LA*-L1-L2 completely blocks the entrance to the catalytic site. Loop L2 in particular is bent into a conformation that closes the active site, a feature that has not been reported previously. The resulting twist of the active-site loops impedes proper adjustment of the catalytic triad and formation of the oxyanion hole, as well as the S1 specificity pocket. Thus the protease domain of the DegP chaperone is present in an inactive state, in which substrate binding as well as catalysis is prevented. Furthermore, the widely conserved disulphide bond connecting loops L1 and L2 (Cys 191–Cys 220) is absent. This disulphide is believed to fix the relative orientations of both loops, thereby stabilizing the conformation of the S1 pocket. In DegP, loop LA* fulfills a similar role and represents a flexible, non-covalent link between the two substrate-binding loops L1 and L2. To adopt the classical catalytic model of serine proteases, these loops have to undergo large conformational changes. Structural flexibility of these elements shown by their increased thermal motion factors might facilitate this process.

Escherichia coli DegP has the ability to stabilize a number of non-native proteins *in vivo* and *in vitro*[2,20]. Possible binding sites for misfolded proteins are located within the inner cavity and are constructed entirely by residues of the protease domain. The solvent-accessible height of this chamber is 15 Å at its centre and increases to 18 Å near the outer entrance. Owing to these geometric constrictions, substrates must be partially unfolded to reach the active site (Fig. 4a). As in other chaperones of known structure, the DegP cavity is lined by hydrophobic residues, most of which are conserved. In both trimeric rings, three large hydrophobic grooves are organized around the central Gln 206/Arg 207 cluster and extend towards the PDZ1 domain (Fig. 4b). The hydrophobic grooves are mainly constructed by residues of loop LA and L2. A second potential binding site was observed on the internal side of the three pillars of the cavity. Furthermore, the hydrophobic binding sites of the PDZ1 domains are properly oriented to augment the number of potential binding patches. The alternating arrangement of polar and hydrophobic surfaces, both within one trimeric ring and between trimeric rings, should form the basis for binding exposed hydrophobic side chains and the peptide backbone atoms of substrates. Thus, the ceilings of the DegP cavity may represent docking platforms for partially denatured proteins, a construction reminiscent of a compactor (Fig. 4a). Both docking platforms are structurally flexible, as indicated by their backbone variations and by their high thermal motion factors. This plasticity should allow binding of diverse polypeptides.

Cage-forming proteases and chaperones can be energy dependent or energy independent. In the former group, ATPase activity is important for recognition of target proteins, their dissociation and unfolding, their translocation within the complex, and various gating mechanisms. The crystal structure indicates why these functions are not relevant for DegP. DegP preferably degrades substrates, which are, *per se*, partially unfolded and which might accumulate under extreme conditions[4,21,22]. Alternatively, threading of substrate through the inner chamber could promote unfolding into an extended conformation. Removal of higher-order structural elements would allow the substrate to re-initiate folding after exit from DegP. Recruitment of PDZ domains for the gating mechanism should permit a direct coupling of substrate binding and translocation within the DegP particle. Accordingly, the PDZ domains may function as tentacular arms capturing substrates and transferring them into the inner cavity. By binding to the C terminus or a β-hairpin loop of a protein, the PDZ domains could properly position the substrate for threading it into the central cavity. After accessing this chamber, the fate of the unfolded protein depends on the interplay of loops LA, L1 and L2. □

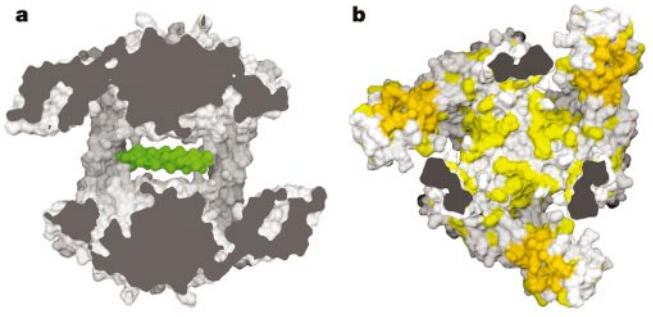

Figure 4 The central cavity. To demonstrate the structural properties of the inner cavity, cleaved presentations of molecule A were generated. Cut regions are shown in black. **a**, Surface representation of the internal tunnel (side view) illustrating its molecular sieve character. Access is restricted to single secondary structure elements as shown by the modelled polyalanine helix (green). **b**, Formation of the hydrophobic-binding patches within the cavity (top view). Hydrophobic residues of the protease domain are shown in yellow, and the non-polar peptide-binding groove of PDZ1 is in orange.

Methods

Crystallization and structure solution

Recombinant his-tagged protein was produced with *E. coli* strain CLC198 (*ΔdegP*::Tn*10*), as described previously[2]. The three-step purification procedure included NiNTA, hydroxylapathite and gel filtration chromatography. Both S210A and S210A-SeMet proteolytically inactive mutants were crystallized at 18 °C using the vapour diffusion method and 10% isopropanol, 10% polyethylene glycol (PEG) 2000 monomethyl ether (MME), 0.1 M Tris/HCl, pH 8.5, as crystallization solution. Hexagonal crystal plates appeared within two weeks and belonged to space group $P6_322$ with cell parameters $a = 121.3$ Å, $b = 121.3$ Å, $c = 237.2$ Å, corresponding to two monomers per asymmetric unit. For a two-day soak with a saturated Ta_6Br_{14} solution, difference Patterson analyses yielded two tantalum sites, which then enabled us to identify four platinum sites in $PtCl_4$-soaked crystals. Subsequently, difference Fourier analyses yielded 21 out of the 28 theoretical selenium sites of SeMet crystals. However, the diffraction pattern of all DegP crystals was extremely anisotropic, restricting data collection to 4.5 Å resolution. This problem could be overcome by transferring crystals to 4 °C and exchanging the reservoir solution by 12% isopropanol, 50% PEG 2000 MME, 0.1 M Tris/HCl, pH 8.5. After one week, the equilibrated crystals could be flash frozen directly in liquid nitrogen. This treatment resulted in an isotropic diffraction pattern to 2.8 Å resolution. A complete multiwavelength anomalous diffraction experiment was performed with the SeMet crystals at the high-brilliance beamline ID14-4 at the European Radiation Synchrotron Facility (ERSF; Supplementary Information Table 2).

Model building and refinement

Energy-restrained crystallographic refinement was carried out with maximum likelihood algorithms implemented in CNS[23], using the protein parameters of ref. 24. Bulk solvent, overall anisotropic *B*-factor corrections and non-crystallographic restraints were introduced depending on the behaviour of the R_{free} index. Refinement proceeded in several cycles, which were interrupted for manual rebuilding with the program O[25]. After the addition of solvent molecules, the refinement converged at an *R*-factor of 21.8% (R_{free} = 27.5%). We prepared all graphical presentations using the programs MOLSCRIPT[26], RASTER3D[27], SETOR[28], GRASP[29] and DINO (http://www.dino3d.org).

Received 21 November 2001; accepted 14 February 2002.

1. Wickner, S., Maurizi, M. R. & Gottesman, S. Posttranslational quality control: folding, refolding, and degrading proteins. *Science* **286,** 1888–1893 (1999).
2. Spiess, C., Beil, A. & Ehrmann, M. A temperature-dependent switch from chaperone to protease in a widely conserved heat shock protein. *Cell* **97,** 339–347 (1999).
3. Gottesman, S., Wickner, S. & Maurizi, M. R. Protein quality control: triage by chaperones and proteases. *Genes Dev.* **11,** 815–823 (1997).
4. Lipinska, B., Zylicz, M. & Georgopoulos, C. The Htra (Degp) protein, essential for *Escherichia coli* survival at high temperatures, is an endopeptidase. *J. Bacteriol.* **172,** 1791–1797 (1990).
5. Pallen, M. J. & Wren, B. W. The HtrA family of serine proteases. *Mol. Microbiol.* **26,** 209–221 (1997).
6. Zumbrunn, J. & Trueb, B. Primary structure of a putative serine protease specific for IGF-binding proteins. *FEBS Lett.* **398,** 187–192 (1996).
7. Gray, C. W. *et al.* Characterization of human HtrA2, a novel serine protease involved in the mammalian cellular stress response. *Eur. J. Biochem.* **267,** 5699–5710 (2000).
8. Suzuki, Y. *et al.* A serine protease, HtrA2, is released from the mitochondria and interacts with XIAP, inducing cell death. *Mol. Cell* **8,** 613–621 (2001).
9. Wootton, J. C. & Drummond, M. H. The Q-Linker—a class of interdomain sequences found in bacterial multidomain regulatory proteins. *Protein Eng.* **2,** 535–543 (1989).
10. Cabral, J. H. M. *et al.* Crystal structure of a PDZ domain. *Nature* **382,** 649–652 (1996).
11. Liao, D. I., Qian, J., Chisholm, D. A., Jordan, D. B. & Diner, B. A. Crystal structures of the photosystem II D1 C-terminal processing protease. *Nature Struct. Biol.* **7,** 749–753 (2000).
12. Lowe, J. *et al.* Crystal structure of the 20s proteasome from the archaeon *T. acidophilum* at 3.4 Å resolution. *Science* **268,** 533–539 (1995).
13. Bochtler, M., Ditzel, L., Groll, M. & Huber, R. Crystal structure of heat shock locus V (HslV) from *Escherichia coli*. *Proc. Natl Acad. Sci. USA* **94,** 6070–6074 (1997).
14. Wang, J. M., Hartling, J. A. & Flanagan, J. M. The structure of ClpP at 2.3 Å resolution suggests a model for ATP-dependent proteolysis. *Cell* **91,** 447–456 (1997).
15. Larsen, C. N. & Finley, D. Protein translocation channels in the proteasome and other proteases. *Cell* **91,** 431–434 (1997).
16. Groll, M. *et al.* A gated channel into the proteasome core particle. *Nature Struct. Biol.* **7,** 1062–1067 (2000).
17. Brandstetter, H., Kim, J. S., Groll, M. & Huber, R. Crystal structure of the tricorn protease reveals a protein disassembly line. *Nature* **414,** 466–470 (2001).
18. Doyle, D. A. *et al.* Crystal structures of a complexed and peptide-free membrane protein-binding domain: molecular basis of peptide recognition by PDZ. *Cell* **85,** 1067–1076 (1996).
19. Songyang, Z. *et al.* Recognition of unique carboxyl-terminal motifs by distinct PDZ domains. *Science* **275,** 73–77 (1997).
20. Misra, R., Castillokeller, M. & Deng, M. Overexpression of protease-deficient DegP(S210A) rescues the lethal phenotype of *Escherichia coli* OmpF assembly mutants in a degP background. *J. Bacteriol.* **182,** 4882–4888 (2000).
21. Swamy, K. H. S., Chung, C. H. & Goldberg, A. L. Isolation and characterization of protease Do from *Escherichia coli*, a large serine protease containing multiple subunits. *Arch. Biochem. Biophys.* **224,** 543–554 (1983).
22. Strauch, K. L., Johnson, K. & Beckwith, J. Characterization of *degP*, a gene required for proteolysis in the cell envelope and essential for growth of *Escherichia coli* at high temperature. *J. Bacteriol.* **171,** 2689–2696 (1989).
23. Brunger, A. T. *et al.* Crystallography & NMR system: a new software suite for macromolecular structure determination. *Acta Crystallogr. D* **54,** 905–921 (1998).
24. Engh, R. A. & Huber, R. Accurate bond and angle parameters for X-ray protein-structure refinement. *Acta Crystallogr. A* **47,** 392–400 (1991).
25. Jones, T. A., Zou, J. Y., Cowan, S. W. & Kjeldgaard, M. Improved methods for building protein models in electron density maps and the location of errors in these models. *Acta Crystallogr. A* **47,** 110–119 (1991).
26. Kraulis, P. J. Molscript—a program to produce both detailed and schematic plots of protein structures. *J. Appl. Crystallogr.* **24,** 946–950 (1991).
27. Merritt, E. A. & Bacon, D. J. in *Macromolecular Crystallography* Part B 505–524 (Methods in Enzymology, Vol. 277, Academic, New York, 1997).
28. Evans, S. V. Setor—hardware-lighted 3-dimensional solid model representations of macromolecules. *J. Mol. Graph.* **11,** 134–138 (1993).
29. Nicholls, A., Bharadwaj, R. & Honig, B. Grasp—graphical representation and analysis of surface properties. *Biophys. J.* **64,** A166–A166 (1993).
30. Perona, J. J. & Craik, C. S. Structural basis of substrate specificity in the serine proteases. *Protein Sci.* **4,** 337–360 (1995).

Supplementary Information accompanies the paper on *Nature's* website (http://www.nature.com).

Acknowledgements

We thank C. Spiess for providing cells for SeMet expression, and G. P. Bourenkov and J. McCarthy for assistance during data collection at beamlines BW6 (DESY, Hamburg) and ID14-4 (ESRF, Grenoble), respectively. We thank R. A. John and W. Bode for critical reading of the manuscript. Financial support by EU ERB (M.G.-F.), DFG (R.H.) and Aventis (T.C.) is acknowledged.

Competing interests statement

The authors declare that they have no competing financial interests.

Correspondence and requests for materials should be addressed to T.C. (e-mail: clausen@biochem.mpg.de). The atomic coordinates and structure factor amplitudes of the DegP S210A crystal structure have been deposited at the Protein Data Bank under entry code 1KJ9.

enzyme is not required for this proton pumping in the reductive phase. Proton pumping only occurs on injection of the second electron. This is notable because in the oxidative phase of the cycle a single electron seems to be sufficient, and may indicate that more redox energy per electron is available in the oxidative part of the cycle. The usage of the proton transfer pathways is partially different. The charge-compensating proton appears to be taken up by means of the K-pathway in the E to R transition (in contrast to the prediction of ref. 4), but through the D-pathway in the F to O transition (Fig. 2b and ref. 21). The D-pathway, however, is required for proton pumping in both cases. The mechanism of proton-pumping itself remains to be elucidated. □

Methods

The proteoliposomes of wild-type or D124N cytochrome *c* oxidase were prepared as described[9]. For the spectroscopic measurements, 500 µl proteoliposomes containing 6 µM or 20 µM enzyme were mixed with 500 µl of 50 mM HEPES/KOH buffer, pH 7.4, 100 mM β-D-glucose in an anaerobic cuvette, degassed and overlaid with argon. After recording a reference spectrum for the oxidized form of the enzyme (O), a 100-fold molar excess of hydrogen peroxide and 40 µg glucose oxidase were added to form state F. Next, we added 25 µg catalase, and the cuvette was flushed with carbon monoxide in the dark. We recorded optical absorbance spectra every 90 s. For comparison the same procedure was used with 10 µM solubilized D124N mutant enzyme in the presence of 0.05% dodecyl-β-D-maltoside as detergent.

The photopotential was measured as described[9]. Proteoliposomes were adsorbed to a planar lipid membrane (protein concentration in the cuvette approximately 100 nM), and the potential was measured across the proteoliposome/planar membrane system. The states E or F were prepared as described above for the spectroscopic measurements. Next, the cytochrome *c* oxidase was reduced upon laser-flash excitation of tris(2,2′-bipyridyl) ruthenium, a photoactivatable electron donor.

Received 30 July 2001; accepted 18 February 2002.

1. Wikström, M. K. Proton pump coupled to cytochrome *c* oxidase in mitochondria. *Nature* **266,** 271–273 (1977).
2. Wikström, M. Identification of the electron transfers in cytochrome oxidase that are coupled to proton-pumping. *Nature* **338,** 776–778 (1989).
3. Michel, H. The mechanism of proton pumping by cytochrome *c* oxidase. *Proc. Natl Acad. Sci. USA* **95,** 12819–12824 (1998).
4. Michel, H. Cytochrome *c* oxidase: catalytic cycle and mechanisms of proton pumping—a discussion. *Biochemistry* **38,** 15129–15140 (1999).
5. Verkhovsky, M. I., Jasaitis, A., Verkhovskaya, M. L., Morgan, J. E. & Wikström, M. Proton translocation by cytochrome *c* oxidase. *Nature* **400,** 480–483 (1999).
6. Ferguson-Miller, S. & Babcock, G. T. Heme/copper terminal oxidases. *Chem. Rev.* **96,** 2889–2907 (1996).
7. Michel, H., Behr, J., Harrenga, A. & Kannt, A. Cytochrome *c* oxidase: structure and spectroscopy. *Annu. Rev. Biophys. Biomol. Struct.* **27,** 329–356 (1998).
8. Nilsson, T. Photoinduced electron transfer from tris(2,2′-bipyridyl)ruthenium to cytochrome *c* oxidase. *Proc. Natl Acad. Sci. USA* **89,** 6497–6501 (1992).
9. Ruitenberg, M. *et al.* Single-electron reduction of the oxidized state is coupled to proton uptake via the K pathway in *Paracoccus denitrificans* cytochrome *c* oxidase. *Proc. Natl Acad. Sci. USA* **97,** 4632–4636 (2000).
10. Mitchell, R. & Rich, P. R. Proton uptake by cytochrome *c* oxidase on reduction and on ligand binding. *Biochim. Biophys. Acta* **1186,** 19–26 (1994).
11. Iwata, S., Ostermeier, C., Ludwig, B. & Michel, H. Structure at 2.8 Å resolution of cytochrome *c* oxidase from *Paracoccus denitrificans*. *Nature* **376,** 660–669 (1995).
12. Thomas, J. W., Puustinen, A., Alben, J. O., Gennis, R. B. & Wikström, M. Substitution of asparagines for asparate-135 in subunit I of the cytochrome *bo* ubiquinol oxidase of *Escherichia coli* eliminates proton-pumping activity. *Biochemistry* **32,** 10923–10928 (1993).
13. Thomas, J. W., Lemieux, L. J., Alben, J. O. & Gennis, R. B. Site-directed mutagenesis of highly conserved residues in helix VIII of subunit I of the cytochrome *bo* ubiquinol oxidase from *Escherichia coli*: an amphipathic transmembrane helix that may be important in conveying protons to the binuclear center. *Biochemistry* **32,** 11173–11180 (1993).
14. Verkhovsky, M. I., Tuukkanen, A., Backgren, C., Puustinen, A. & Wikström, M. Charge translocation coupled to electron injection into oxidized cytocrome *c* oxidase from *Paracoccus denitrificans*. *Biochemistry* **40,** 7077–7083 (2001).
15. Witt, S. N. & Chan, S. I. Evidence for a ferryl Fea3 in oxygenated cytochrome *c* oxidase. *J. Biol. Chem.* **262,** 1446–1448 (1987).
16. Vygodina, T. V. & Konstantinov, A. A. H_2O_2-Induced conversion of cytochrome *c* oxidase peroxy complex to oxoferryl state. *Ann. NY Acad. Sci.* **550,** 124–138 (1988).
17. Moody, A. J. Ligation and electronation states of cytochrome *c* oxidase in relation to other oxidases and peroxidases. *Biochem. Soc. Trans.* **19,** 617–622 (1991).
18. Greenwood, C., Wilson, M. T. & Brunori, M. Studies on partially reduced mammalian cytochrome oxidase. Reactions with carbon monoxide and oxygen. *Biochem. J.* **137,** 205–215 (1974).
19. Brzezinski, P. & Malmström, B. G. The reduction of cytochrome *c* oxidase by carbon monoxide. *FEBS Lett.* **187,** 111–114 (1985).
20. Oliveberg, M. & Malmström, B. G. Internal electron transfer in cytochrome *c* oxidase: evidence for a rapid equilibrium between cytochrome *a* and the bimetallic site. *Biochemistry* **30,** 7053–7057 (1991).
21. Konstantinov, A. A., Siletsky, S., Mitchell, D., Kaulen, A. & Gennis, R. The roles of two proton input channels in cytochrome *c* oxidase from *Rhodobacter sphaeroides* probed by the effects of site-directed mutations on time-resolved electrogenic intraprotein proton transfer. *Proc. Natl Acad. Sci.USA* **94,** 9085–9090 (1997).
22. Jasaitis, A., Verkhovsky, M. I., Morgan, J. E., Verkhovskaya, M. L. & Wikström, M. Assignment and charge translocation stoichiometries of the major electrogenic phases in the reaction of cytochrome *c* oxidase with dioxygen. *Biochemistry* **38,** 2697–2706 (1999).

Acknowledgements

We thank the Deutsche Forschungsgemeinschaft, the Fonds der Chemischen Industrie and the Max-Planck-Gesellschaft for financial support. We are grateful to B. Ludwig for providing the D124N mutant.

Correspondence and requests for materials should be addressed to H.M. (e-mail: michel@mpibp-frankfurt.mpg.de) or K.F. (e-mail: fendler@mpibp-frankfurt.mpg.de).

errata

A laboratory analogue of the event horizon using slow light in an atomic medium

Ulf Leonhardt

Nature **415**, 406–409 (2002).

In Table 1 of this Letter, the average particle number for slow light was incorrectly expressed as: $\frac{1}{(e^{\pi\mu}-e^{-\pi\mu})^2}$. It should have read: $\frac{1}{(e^{\pi\mu}+e^{-\pi\mu})^2}$. □

Cbl–CIN85–endophilin complex mediates ligand-induced downregulation of EGF receptors

Phillippe Soubeyran, Katarzyna Kowanetz, Iwona Szymkiewicz, Wallace Y. Langdon & Ivan Dikic

Nature **416**, 183–188 (2002).

In Fig. 3c of this Letter, the line (filled circles) labelled EGF+CIN85 should have been labelled EGFR+CIN85−3SH3, as in Fig. 3d. □

corrigendum

Crystal structure of DegP (HtrA) reveals a new protease-chaperone machine

Tobias Krojer, Marta Garrido-Franco, Robert Huber, Michael Ehrmann & Tim Clausen

Nature **416**, 455–459 (2002).

In this Letter, the Protein Data Bank entry code for the DegP S210A crystal structure is incorrectly listed as 1KJ9. It should be 1KY9. We thank C. Zardecki for bringing this to our attention. □